IOPscience iopscience.iop.org

Home Search Collections Journals About Contact us My IOPscience

A quantum correction Poisson equation for metal–oxide–semiconductor structure simulation

This content has been downloaded from IOPscience. Please scroll down to see the full text.

2004 Semicond. Sci. Technol. 19 917

(http://iopscience.iop.org/0268-1242/19/7/024)

View the table of contents for this issue, or go to the journal homepage for more

Download details:

IP Address: 140.113.38.11

This content was downloaded on 28/04/2014 at 00:05

Please note that terms and conditions apply.

Semicond. Sci. Technol. **19** (2004) 917–922 PII: S0268-1242(04)75094-4

# A quantum correction Poisson equation for metal–oxide–semiconductor structure simulation

**Yiming Li**

Department of Computational Nanoelectronics, National Nano Device Laboratories, Hsinchu 300, Taiwan
and
Microelectronics and Information Systems Research Center, National Chiao Tung University, Hsinchu 300, Taiwan

Received 23 January 2004
Published 8 June 2004
Online at stacks.iop.org/SST/19/917
doi:10.1088/0268-1242/19/7/024

**Abstract**
In this paper, we present a quantum correction Poisson equation for metal–oxide–semiconductor (MOS) structures under inversion conditions. Based on the numerical solution of Schrödinger–Poisson (SP) equations, the new Poisson equation developed is optimized with respect to (1) the position of the charge concentration peak, (2) the maximum of the charge concentration, (3) the total inversion charge sheet density $Q$, and (4) the average inversion charge depth $X$. Instead of solving a set of coupled SP equations, this physically-based Poisson equation characterizes the quantum confinement effects of the MOS structure from the interface of silicon and oxide ($Si/SiO_2$) with the silicon substrate. It successfully predicts distribution of the electron density in inversion layers for MOS structures with various oxide thicknesses $T_{ox}$ and applied gate voltages $V_G$. Compared to SP results, the prediction of the proposed equation is within 3% accuracy. Application of this equation to the capacitance–voltage measurement of an n-type metal–oxide–semiconductor field effect transistor (MOSFET) produces an excellent agreement. This quantum correction Poisson equation can be solved together with transport equations, such as drift-diffusion, hydrodynamic and Boltzmann transport equations without encountering numerical difficulties. It is feasible for nanoscale MOSFET simulation.

## 1. Introduction

Development of advanced MOSFETs has been of great interest in recent years [1–32]. As the dimensions of MOSFETs are further scaled into the nanoscale regime [1–5], oxide thickness in a MOSFET can be as thin as 1 nm, prevented only by the leakage tunnelling current [6–8]. For the oxide thickness ($T_{ox}$) of 1–3 nm and the applied gate voltage ($V_G$) of 0.5–1.5 V, the displacement of the inversion carrier density shifts away from the $Si/SiO_2$ interfaces due to the quantization effect [9–27]. It becomes important to consider quantum-mechanical effects when performing nanoscale semiconductor device modelling and simulation; in particular any accurate calculations of the inversion-layer capacitance must take this quantization effect into consideration [6–27]. Various theoretical approaches have been considered to study the quantum confinement effects, such as full quantum-mechanical model and quantum corrections to the drift-diffusion, hydrodynamic and Boltzmann transport models [9–27].

As shown in figure 1, the most accurate way of incorporating the quantum confinement effects in the inversion layers of a MOS structure is to solve a set of coupled Schrödinger–Poisson equations from the interface of $Si/SiO_2$ with the silicon substrate (i.e., along the $z$-axis) subject to an appropriate boundary condition [9–15], but this encounters numerical difficulties and is a time-consuming task in nanoscale MOSFET device simulation [11–14]. For most quantum correction models, the classical carrier concentration is directly multiplied by an additional correction term [16–20].

 © 2004 IOP Publishing Ltd Printed in the UK 

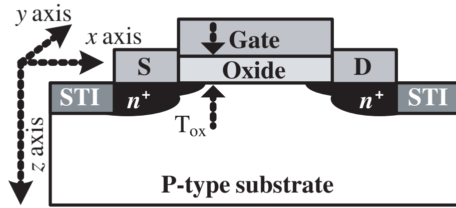


**Figure 1.** A cross-section view of n-type MOSFET.

Meanwhile, other quantum correction approaches have been proposed, such as solving additional differential equation for the gradient of electron density [14, 21–23] or transforming the classical potential into an effective potential by considering an integral transformation [24–27], therefore, electron density is corrected by the new quantum corrected potential. Either numerical difficulties or quantitatively incorrect estimations have been encountered in these approaches [23, 27]. We have recently proposed new quantum correction models based on high-order term approximation for nanoscale MOSFET device simulation [19, 20]. However, to establish a physically more proper quantum correction to carrier density in the interface of $Si/SiO_2$ self-consistently, it is necessary to directly model the quantum potential by considering a new Poisson equation.

Based on a phenomenological investigation from the numerical solution of SP equations, the source term on the right-hand side of the classical Poisson equation is reformulated using an intelligent computation algorithm [28]. The developed quantum correction Poisson equation is mainly optimized with respect to four physical constraints (1) the position of the charge concentration peak, (2) the maximum of the charge concentration, (3) the total inversion charge sheet density $Q$, and (4) the average inversion charge depth $X$. It can be solved directly to reflect the quantum confinement effect, and successfully predicts distribution of the electron density in inversion layers for MOS structures with various oxide thicknesses and applied gate voltages. In the numerical solution of such nonlinear Poisson equations, both Newton and monotone iterative methods [29] are used to solve this new quantum correction Poisson equation, and have good convergence properties. Among different quantum correction models, such as Hänsch, MLDA, effective potential, density-gradient model, the calculation result with our model is most close to SP results for a MOS structure simulation [14–27]. Compared to the SP results, prediction of the proposed equation is within 3% accuracy. Application of this equation to the calculation of capacitance–voltage (CV) curves for an n-type MOSFET produces an excellent agreement on the measured data. This quantum correction Poisson equation can be solved together with transport equations, such as drift-diffusion, hydrodynamic and Boltzmann transport equations [30–32] without encountering numerical difficulties. We believe that by using this new quantum correction Poisson equation, the conventional transport models above can directly apply to the nanoscale MOSFET simulation.

This paper is organized as follows. In section 2, we state the proposed quantum correction Poisson equation. Section 3 shows the simulation results. Comparisons of the new equation and SP equations on the quantum potential and electron density are discussed. A simulated CV curve is compared with the measured data. Section 4 draws the conclusions.

## 2. Quantum correction Poisson equation

As shown in figure 1, a poly-oxide-silicon MOS structure is simulated with the coupled SP equations self-consistently along the longitudinal direction ($z$-axis) from the interface of $Si/SiO_2$ with the silicon substrate [9–15]. For simplicity in the model construction, the SP equations considered here are assumed to have no wave penetration at the interface of $Si/SiO_2$ [9–15]. SP equations are discretized by the finite volume method [13, 14, 29]. After the discretization, the corresponding matrix eigenvalue problem and the system of nonlinear algebraic equations are solved iteratively to obtain a self-consistent solution [9–15]. More than 30 sub-bands are calculated in the numerical solution of the Schrödinger equation [13, 14].

For nanoscale MOSFET devices with ultrathin oxide, the chosen $T_{ox}$ varies from 1 to 3 nm and the applied $V_G$ ranges from 0.5 V to 1.5 V. For MOS structures under inversion conditions, we consider the electron density from the interface of $Si/SiO_2$ to the silicon bulk completely. In the modelling, a poly-$SiO_2$–Si MOS structure is tested with the classical transport approximation and SP solution self-consistently. Thirty-two sub-bands are computed in the solution of the Schrödinger equation. The formulated electron density $n$ in the quantum correction Poisson equation is

$$\nabla \cdot (\varepsilon \nabla \phi) = -q\left(p - n + N_D^+ - N_A^-\right) \tag{1}$$

$$n = a_0 \frac{2N_C}{\sqrt{\pi}}\left(1 - \exp\left(-a_1\xi^2 + a_2\xi^3 - a_3\xi^4\right)\right)F \tag{2}$$

where $N_C$ is the effective density of state in the conduction band, $F$ is the Fermi–Dirac integral [15, 29–31], and $\xi = x/\lambda_{th}$ and $\lambda_{th}$ is the thermal wavelength [9–27]. $q = 1.602\,18 \times 10^{-19}$ C is the elementary charge and $\varepsilon = 11.9\varepsilon_0$ is the silicon permittivity. $n$ and $p$ are the densities of free electrons and holes, respectively; $N_D^+$ and $N_A^-$ are the ionized donor and acceptor impurities doping concentrations, respectively; and $\varepsilon_0 = 8.854\,18 \times 10^{-14}$ F cm$^{-1}$ is the permittivity in vacuum [15, 29–31]. For the hole density $p$, we only consider Boltzmann statistics [15, 29–31]. Using a genetic algorithm, the four model parameters $a_0$–$a_3$ are optimized to best fit the self-consistent SP solution for all different $T_{ox}$ and $V_G$. The chosen $T_{ox}$ varies from 1 to 3 nm and the applied $V_G$ ranges from 0.5 to 1.5 V. This intelligent computation algorithm has been proposed for optimal characterization of different semiconductor devices in our recent work [28].

After optimization, these parameters can be formulated as a function of surface quantum potential $\phi$ as follows:

$$a_0 = -1.65 + 2.98\phi \tag{3}$$

$$a_1 = -2.9 + 3.075\phi \tag{4}$$

$$a_2 = 78.689 - 218.158\phi + 199.696\phi^2 - 60.233\phi^3, \tag{5}$$

and

$$a_3 = -0.2539 + 0.2548\phi. \tag{6}$$

The model parameters $a_0$–$a_3$ shown in figures 2–5 are based on a MOS with p-type substrate and substrate doping $N_A^- = 10^{17}$ cm$^{-3}$. The lines are our models that are the fitted formulae for parameters $a_0$–$a_3$, the symbols are optimal data calibrated with SP results, and $\phi_s$ is the surface quantum potential

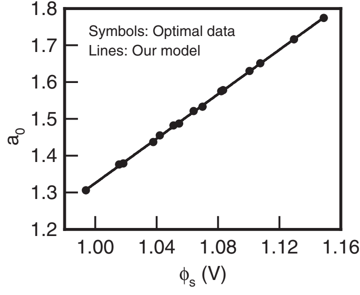


**Figure 2.** Plot of the coefficient $a_0$. The symbols are the optimal data obtained from the SP equations. The solid line is the fitted formula, our model, for the coefficient $a_0$.

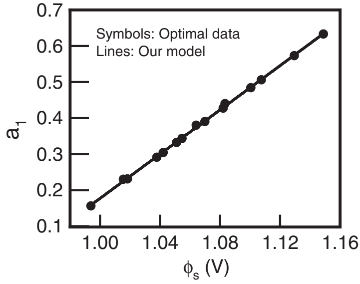


**Figure 3.** Plot of the coefficient $a_1$.

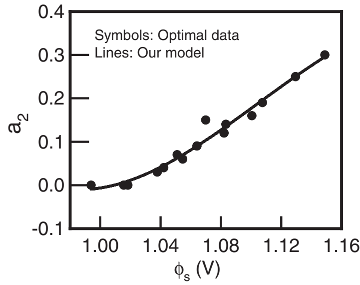


**Figure 4.** Plot of the coefficient $a_2$.

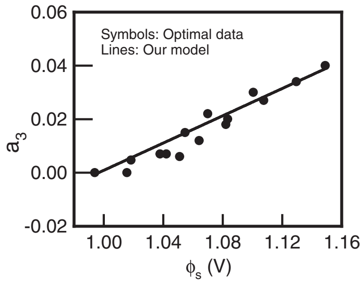


**Figure 5.** Plot of the coefficient $a_3$.

solved from the quantum correction Poisson equation shown in figures 2–5. $a_0$ and $a_1$ linearly depend on $\phi$, $a_2$ shows a nonlinear relationship with $\phi$ and goes to zero when $\phi$ approaches 1 V. $a_3$ has a small variation range and approaches zero when $\phi$ approaches 1 V.

The accuracy of the proposed quantum correction Poisson equation to the data in terms of (1) the position of the charge concentration peak, (2) the maximum of the charge concentration, (3) the total inversion charge sheet density

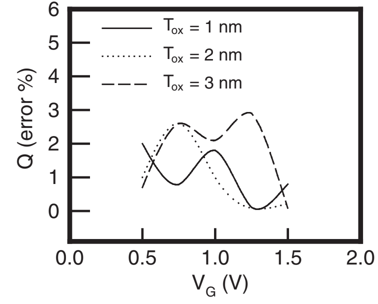


**Figure 6.** Error plots of the total inversion charge sheet density $Q$ with respect to different $T_{\mathrm{ox}}$ and $V_{\mathrm{G}}$.

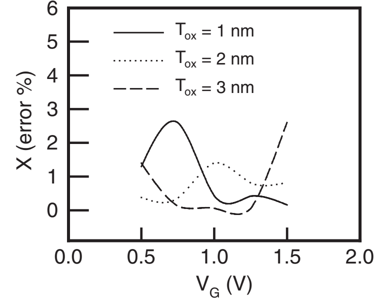


**Figure 7.** Error plots of the average inversion charge depth $X$ with respect to different $T_{\mathrm{ox}}$ and $V_{\mathrm{G}}$.

$Q = \int_0^\infty n(z)\,\mathrm{d}z$, and (4) the average inversion charge depth $X = \int_0^\infty zn(z)\mathrm{d}z \big/ \int_0^\infty n(z)\,\mathrm{d}z$ is within 3%. For example, figures 6 and 7 show relative errors between the results of our equation and SP equations for the computed total inversion charge sheet density $Q$ and the average inversion charge depth $X$, respectively. They are less than 3% for the simulated MOS with respect to different $T_{\mathrm{ox}}$ and $V_{\mathrm{G}}$. For other substrate doping profiles, we may slightly adjust the applied gate voltage to meet the shift in the threshold voltage due to the change in $N_{\mathrm{A}}^{-}$. We note that the right-hand side of the proposed quantum correction Poisson equation is similar to the term on the right-hand side of the classical Poisson equation [15, 29–31]. The quantum correction Poisson equation can be discretized with, for example, finite difference, finite element, or finite volume methods [33], and the discretized differential equation leads to a system of nonlinear algebraic equations. Numerically we have successfully solved the corresponding system of nonlinear algebraic equations using both Newton and monotone iterative methods without encountering any numerical difficulties [13, 14, 29, 31, 32].

## 3. Results and discussion

For the n-MOS with different $T_{\mathrm{ox}}$ and gate voltage $V_{\mathrm{G}}$, figures 8–11 present the calculated potential and electron density by using the SP equations, the classical Poisson equation [15, 29–31], and the quantum correction Poisson equation along with the optimal data and our model for coefficients $a_0$–$a_3$. The optimal data mean using all optimized values (calibrated with SP results) for the four parameters $a_0$–$a_3$ in the quantum correction Poisson equations (1), (2). Our model is the quantum correction Poisson equations (1), (2)

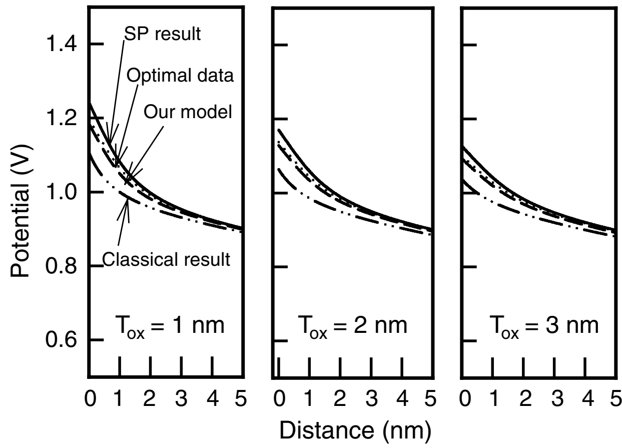


**Figure 8.** Computed potential with the classical Poisson, SP, optimal data, and our model, where $V_G = 1$ V.

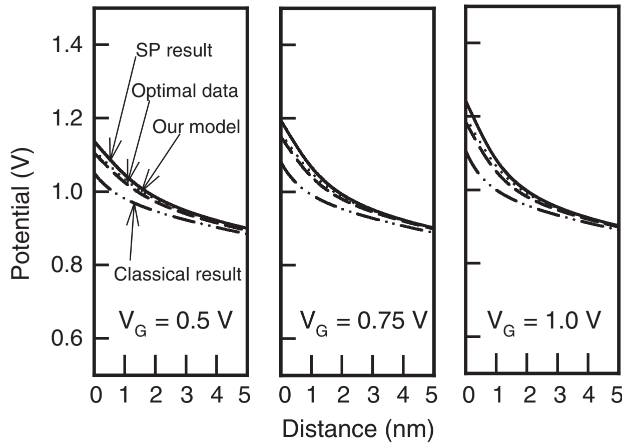


**Figure 9.** Computed potential with the classical Poisson, SP, optimal data, and our model, where $T_{ox} = 1$ nm.

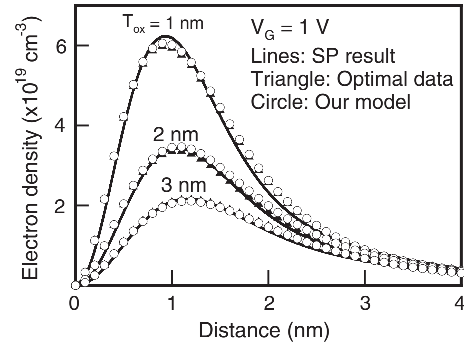


**Figure 10.** Computed electron densities with SP, optimal data, and our model, where $V_G = 1$ V.

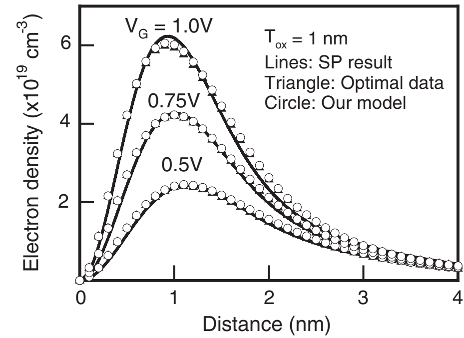


**Figure 11.** Computed electron densities with SP, optimal data, and our model, where $T_{ox} = 1$ nm.

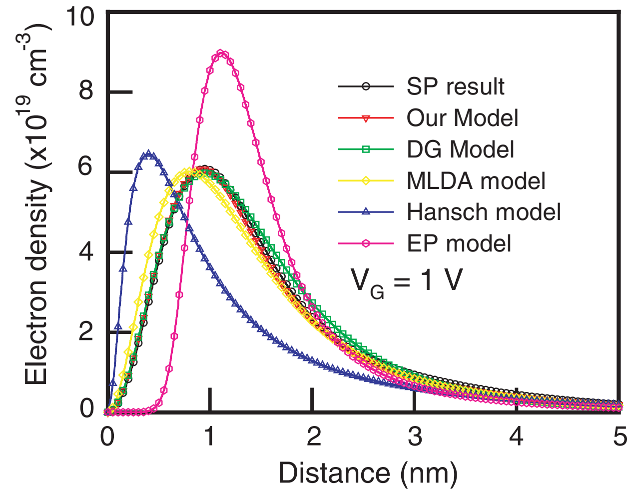


**Figure 12.** Comparison of the distribution of the electron density with different quantum correction models.

with formulae (3), (6). For the simulated MOS, figure 8 reports the computed potential distribution (along distance $z$-axis) with the classical Poisson, SP, optimal data and our model, where $T_{ox}$ varies from 1 nm (the left figure) to 3 nm (the right one) and $V_G = 1$ V is fixed. At the interface of $Si/SiO_2$ (i.e., distance $z = 0$ nm), the potential difference between our model and the SP result is less than $0.5V_T$ ($V_T$ is thermal voltage [30, 31] and is equal to 0.0259 V at room temperature). However, the difference between the classical Poisson and SP result is equal to $5V_T \approx 0.1$ V. Similarly, figure 9 is the computed potential distribution with the classical Poisson, SP, optimal data and our model, where $V_G$ is from 0.5 V (the left figure) to 1.0 V (the right one) and $T_{ox}$ is fixed at 1 nm. Both figures confirm that the proposed quantum correction Poisson equation together with the modelled parameters demonstrate good agreement with the SP results.

With the computed potential, we calculate the corresponding electron density with respect to different $T_{ox}$ and $V_G$, shown in figures 10 and 11. Classical electron density attains maximum value at the interface of $Si/SiO_2$, which is significantly different from the quantum-mechanical results [9–14]. Therefore, we focus here only on the comparison of the results of the quantum correction Poisson equation and SP equations. Figure 10 shows the computed electron densities with SP, optimal data and our model, where $T_{ox} = 1$–3 nm and $V_G = 1$ V. The results clearly show good accuracy between the models. Similarly, figure 11 shows the computed electron densities with SP, optimal data and our model, where $V_G = 0.5$, 0.75 and 1.0 V, and $T_{ox} = 1$ nm. Peak value and peak position of the distribution of electron density are in good agreement on the result of the SP equations.

Furthermore, we carefully explore the accuracy of the distribution of electron density of our model by comparing

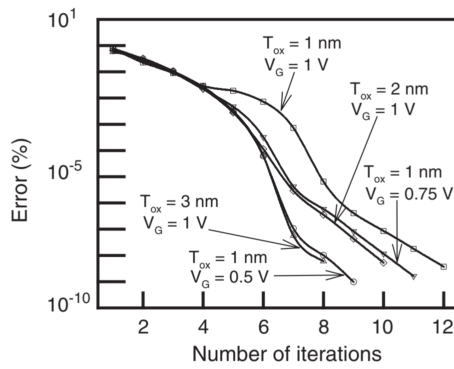


**Figure 13.** Convergence property of the numerical solution of the quantum correction Poisson equation using a typical Newton method.

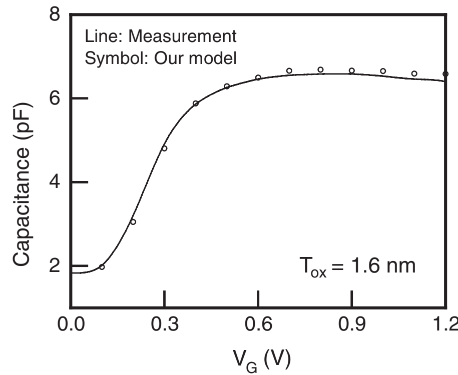


**Figure 14.** Simulated and measured CV curves for the n-type MOSFET with $T_{ox} = 1.6$ nm.

with several well-known quantum correction models: Hänsch [16], MLDA [17], effective potential (EP) [24, 25], density-gradient (DG) [21] and SP [9–15] models. The simulated MOS is with the uniform doping profile $N_A^- = 10^{17}$ cm$^{-3}$, $T_{ox} = 1$ nm and $V_G = 1$ V. Figure 12 shows the comparison among these different models. Electron densities calculated with Hänsch (blue triangle) and EP (pink circle) models are significantly different from SP (black circle) result [27]. The DG model requires solution of additional auxiliary differential equation, which involves special numerical treatment on the discretization of DG equation [23]. Among different quantum correction models, the calculation result with our model is most close to the SP results for the MOS structure simulation. By using a typical Newton's method [31], the convergence property of the numerical solution of the quantum correction Poisson equation is also examined. Figure 13 shows the achieved convergence behaviour for the numerical solution of the finite volume discretized quantum correction Poisson with respect to different $T_{ox}$ and $V_G$. For the MOS with $T_{ox} = 1$ nm, it takes 9, 11 and 12 iterations to meet the specified stopping criterion (error $< 10^{-8}$) for $V_G = 0.5$ V, 0.75 V and 1 V, respectively. For other $T_{ox}$ and $V_G$, similar convergence behaviour has also been obtained, as shown in figure 13.

We apply this quantum correction Poisson equation to calculate CV curve of an n-type MOSFET and compare with the measured data. A $20 \times 20$ $\mu$m$^2$ n-type MOSFET with uniform substrate doping profile $N_A^- = 10^{17}$ cm$^{-3}$ and $T_{ox} =$ 1.6 nm is fabricated and measured for the investigation of the CV curve. The CV curve of the MOSFET sample is measured at a frequency of 100 kHz. Details of the experiment were reported in our recent work [19]. The experimentally measured data are shown together with our result in figure 14. The capacitance consists of three components in series connection: the poly-gate capacitance, the gate-oxide capacitance and the surface capacitance. The agreement is excellent except for $V_G > 1.2$ V. This is expected as we have assumed zero penetration of the wavefunction into the oxide in our SP solver and model formulation. The deviation of the calculated result from the measured data indicates that there is a substantial gate tunnelling current through the oxide taking place at $V_G > 1.2$ V [7, 11, 15, 19].

## 4. Conclusions

In this paper, based on SP solutions we have developed a new quantum correction Poisson equation for ultrathin MOS structures under inversion condition. Our primary simulations and comparisons on electron density and CV curves have shown the accuracy of this new Poisson equation under different biasing conditions. Compared to SP results, prediction of the proposed equation is within 3% of accuracy. The proposed model provides a novel alternative for nanoscale MOSFET modelling and simulation. Solving this equation with the classical hydrodynamic [31, 32] model for more advanced nanoscale device simulation is under investigation.

## Acknowledgments

This work is supported in part by National Science Council (NSC) of Taiwan under contract numbers: NSC-92-2112-M-429-001 and Ministry of Economic Affairs of Taiwan under contract number PSOC 92-EC-17-A-07-S1-0011.

## References

[1] Chirico F, Della Sala F, Di Carlo A and Lugli P 1999 Quantum effects in nanometer MOS structures *Physica* B **272** 546–9

[2] Sano N, Hiroki A and Matsuzawa K 2002 Device modelling and simulations toward sub-10 nm semiconductor devices *IEEE Trans. Nanotechnol.* **1** 63–71

[3] Ogawa M, Tsuchiya H and Miyoshi T 2003 Quantum electron transport modelling in nano-scale devices *IEICE Trans. Electron.* **E86-C** 363–71

[4] Pei G, Kedzierski J, Oldiges P, Ieong M and Kan E C-C 2002 FinFET design considerations based on 3-D simulation and analytical modelling *IEEE Trans. Electron Devices* **49** 1411–9

[5] Schulz T, Rosner W, Landgraf E, Risch L and Langmann U 2002 Planar and vertical double gate concepts *Solid-State Electron.* **46** 985–9

[6] Roldán J B, Gámiz F, López-Villanueva J A, Carceller J E and Cartujo P 1999 A computational study of the strained-Si MOSFET: a possible alternative for the next century electronics industry *Comput. Phys. Commun.* **121–122** 547–9

[7] Fu Y, Willander M and Lundgren P 2001 Current and capacitance characteristics of a metal–insulator–semiconductor structure with an ultrathin oxide layer *Superlattices Microstruct.* **30** 53–60

[8] Simonetti O, Maurel T and Jourdain M 2002 Characterization of ultrathin metal–oxide–semiconductor structures using coupled current and capacitance–voltage models based on quantum calculation *J. Appl. Phys.* **92** 4449–58
[9] Stern F and Howard W E 1967 Properties of semiconductor surface inversion layers in the electric quantum limit *Phys. Rev.* **163** 816–35
[10] Ando T, Fowler A B and Stern F 1982 Electronics properties of two-dimensional systems *Rev. Mod. Phys.* **54** 437–672
[11] Lo S H, Buchanan D A, Taur Y and Wang W 1997 Quantum-mechanical modeling of electron tunneling current from the inversion layer of ultra-thin oxide nMOSFET's *IEEE Electron Device Lett.* **18** 209–11
[12] Trellakis A, Galick A T, Pacelli A and Ravaioli G 1997 Iteration scheme for the solution of the two-dimensional Schrödinger–Poisson equations in quantum structures *J. Appl. Phys.* **81** 7880–4
[13] Li Y, Chao T-S and Sze S M 2003 A novel parallel approach for quantum effect simulation in semiconductor devices *Int. J. Modelling Simul.* **23** 94–102
[14] Li Y, Lee J-W, Tang T-w, Chao T-S, Lei T-F and Sze S M 2002 Numerical simulation of quantum effects in high-$k$ gate dielectrics MOS structures using quantum-mechanical models *Comput. Phys. Commun.* **147** 214–7
[15] Taur Y and Ning T H 1998 *Fundamentals of Modern VLSI Devices* (New York: Cambridge University Press)
[16] Hänsch W, Vogelsang T, Kircher R and Orlowski M 1989 Carrier transport near the Si/SiO interface of a MOSFET *Solid-State Electron.* **32** 839–49
[17] Paasch G and Ubensee H 1982 A modified local density approximation *Phys. Status Solidi.* b **113** 165–78
[18] Ma Y, Liu L, Deng W, Tian L, Li Z and Yu Z 2000 A new charge model including quantum-mechanical effects in MOS structure inversion layer *Solid-State Electron.* **44** 1697–702
[19] Tang T-w and Li Y 2002 A SPICE-compatible model for nanoscale MOSFET capacitor simulation under the inversion condition *IEEE Trans. Nanotechnol.* **1** 243–6
[20] Li Y, Tang T-w and Yu S-M 2003 A quantum correction model for nanoscale double-gate MOS devices under inversion conditions *J. Comput. Electron.* **2** 491–5
[21] Ancona M G and Tiersten H F 1987 Macroscopic physics of the silicon inversion layer *Phys. Rev.* B **35** 7959–65
[22] Li Y 2002 A computational efficient approach to the numerical solution of density-gradient equations for ultrathin oxide MOS devices *WSEAS Trans. Circuits* **1** 1–6
[23] Tang T-w, Wang X and Li Y 2002 Discretization scheme for the density-gradient equations and effect of boundary conditions *J. Comput. Electron.* **1** 389–93
[24] Ramey S M and Ferry D K 2002 Modeling of quantum effects in ultrasmall FD-SOI MOSFETs with effective potentials and three-dimensional Monte Carlo *Physica* B **314** 350–3
[25] Ferry D K, Ramey S, Shifren L and Akis R 2002 The effective potential in device modeling: the good, the bad and the ugly *J. Comput. Electron.* **1** 59–65
[26] Asenov A, Watling J R, Brown A R and Ferry D K 2002 The use of quantum potentials for confinement and tunnelling in semiconductor devices *J. Comput. Electron.* **1** 503–13
[27] Li Y, Tang T-w and Wang X 2002 Modeling of quantum effects for ultrathin oxide MOS structures with an effective potential *IEEE Trans. Nanotechnol.* **1** 238–42
[28] Li Y, Cho Y-Y, Wang C-S and Huang K-Y 2003 A genetic algorithm approach to InGaP/GaAs HBT parameters extraction and RF characterization *Japan. J. Appl. Phys.* **42** 2371–4
[29] Li Y 2003 A parallel monotone iterative method for the numerical solution of multidimensional semiconductor Poisson equation *Comput. Phys. Commun.* **153** 359–72
[30] Sze S M 2002 *Semiconductor Devices, Physics and Technology* (New York: Wiley)
[31] Selberherr S 1984 *Analysis and Simulation of Semiconductor Devices* (New York: Springer)
[32] Li Y, Sze S M and Chao T-S 2002 A practical implementation of parallel dynamic load balancing for adaptive computing in VLSI device simulation *Eng. Comput.* **18** 124–37
[33] Varga R S 2000 *Matrix Iterative Analysis* (New York: Springer)